NASA CR-173,616

NASA-CR-173616
19840017699

A Reproduced Copy

OF

NASA CR-173,616

Reproduced for NASA

by the

NASA Scientific and Technical Information Facility

CCMS-84-03
VPI-E-83-9

VIRGINIA TECH

CENTER FOR COMPOSITE MATERIALS AND STRUCTURES

Temperature Dependence of Elastic and Strength Properties of T300/5208 Graphite-Epoxy

Scott Milan Milkovich
Carl T. Herakovich

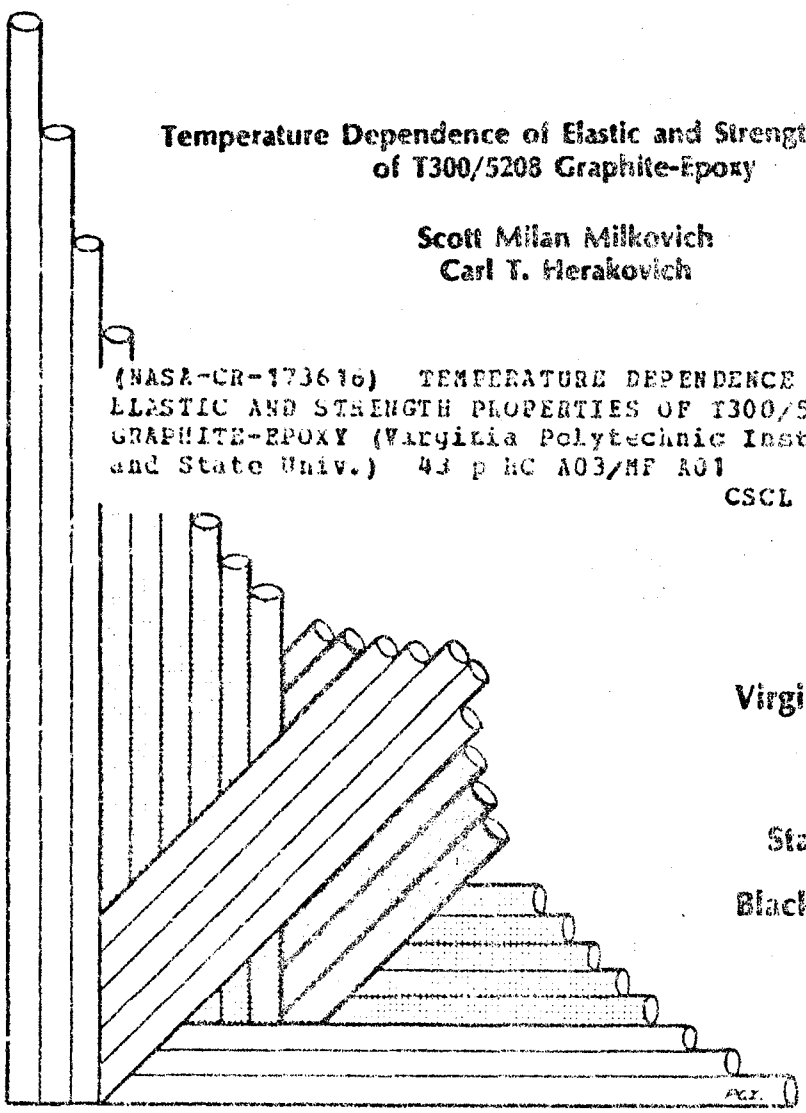

Virginia Polytechnic Institute and State University

Blacksburg, Virginia 24061

College of Engineering

Virginia Polytechnic Institute and State University

Blacksburg, VA 24061

VPI-E-83-9 April, 1984

Temperature Dependence of Elastic and Strength Properties of T300/5208 Graphite-Epoxy

Scott Milan Milkovich[1]
Carl T. Herakovich[2]

Department of Engineering Science & Mechanics

Interim Report 41
The NASA-Virginia Tech Composites Program

NASA Cooperative Agreement NAG-1-343

Prepared for: Applied Materials Branch
National Aeronautics & Space Administration
Langley Research Center
Hampton, VA 23665

[1]Graduate Student

[2]Professor of Engineering Science & Mechanics

ABSTRACT

Experimental results are presented for the elastic and strength properties of T300/5208 graphite-epoxy at room temperature, 116K (-250°F), and 394K (+250°F). Results are presented for unidirectional 0°, 90°, and 45° laminates, and ±30°, ±45°, and ±60° angle-ply laminates. It is shown that the stress-strain behavior of the 0° and 90° laminates is essentially linear for all three temperatures and that the stress-strain behavior of all other laminates is linear at 116K. A second-order curve provides the best fit for the temperature dependence of the elastic modulus of all laminates and for the principal shear modulus. Poisson's ratio appears to vary linearly with temperature. All moduli decrease with increasing temperature except for E_1 which exhibits a small increase. The strength temperature dependence is also quadratic for all laminates except the 0°-laminate which exhibits linear temperature dependence. In many cases the temperature dependence of properties is nearly linear.

1.0 INTRODUCTION

The use of fiber-reinforced composite materials in the aerospace industry has greatly increased in recent years. The great advantage of these materials being their superior strength to weight and stiffness to weight ratios. This makes composite materials ideal for use in space applications. In order to efficiently design structures for use in space, it is necessary to determine the effect of the space-environment on these materials. The cold of space coupled with radiant solar heating effects can lead to a wide range of operating temperatures. Because of this, it is necessary to understand how temperature affects the basic material properties of composite materials.

Obviously, strength and stiffness are two basic material properties which are of fundamental importance. Many proposed applications of fiber-reinforced materials for use in space-environments involve graphite-epoxy composites. This paper presents data on the strength and stiffness properties of T300/5208 graphite-epoxy composite over the temperature range of 116K to 394K (-250°F to +250°F). The designation T300/5208 indicates that the graphite fibers are Thornel (Union Carbide) T300 fibers in a matrix consisting of Narmco 5208 epoxy resin. The temperature range of 116K to 394K represents the temperature extremes that may be encountered in a space-environment [1]. Data, generated from this study, are presented in graphical form (stiffness, strength versus temperature and stress-strain curves) as well as in tabular form. Test procedures are discussed and comments regarding material behavior are injected as warranted.

2.0 PROCEDURE

Test specimens were cut from panels of T300/5208 graphite-epoxy that had been ultrasonicly C-scanned to insure their integrity. The test specimens measured 1.27 centimeters by 25.40 centimeters (0.5 inches by 10.0 inches) and were 1.02 millimeters thick (0.040 inches). .005in/lamina layer This thickness corresponds to 8 lamina layers. Six different laminate lay-up configurations were tested: $[0]_8$, $[45]_8$, and $[90]_8$ (all of which are unidirectional material) as well as $[+30_2/-30_2]_s$, $[+45_2/-45_2]_s$, and $[+60_2/-60_2]_s$. Tabs were not used for load introduction. After allowing for the gripping region, the aspect ratio (length/width) of the test specimens was twelve. Once the specimens had been cut to size, they were placed in a drying oven set at 373K (212°F) for a period of two weeks.

Prior to testing, each composite specimen was fitted with a rectangular (45°) strain-gage rosette. WK-00-120WR-350 (Micro-Measurements, Inc.) strain-gages were used. These gages were choosen because they are designed to withstand large temperature ranges. The gages were mounted using M-Bond 600 adhesive (Micro-Measurements), following the suggested mounting procedure. This procedure includes lightly sanding the composite surface to produce a smooth area were the strain-gage is to be located. Finally wide-temperature range lead wires were attached to the strain-gage rosette (326-GJF, Micro-Measurements).

All tests were performed in an ATS environmental chamber that uses resistance elements for heating and liquid nitrogen for cooling. The heat from the resistance elements is circulated by an internal fan. The liquid nitrogen evaporates as it enters the chamber and is circulated by

a slight overpressure from the nitrogen source. Temperature is monitored throughout the chamber by thermocouples placed at various locations within the chamber, including one thermocouple attached directly to the test specimen. Tests were conducted at three different temperatures: 116K, 301K (room temperature), and 394K. Soak times of four to six hours were required to attain stable conditions at the low test temperture. Two to four hours were required at the high test temperature.

The environmental chamber was mounted on an MTS hydralic tensile testing machine. The tensile machine was fitted with special "moment-free" grips which fit entirely within the chamber [2]. This fixture was designed to provide accurate axial alignment and rotational freedom. Load was measured by a resistance load cell located outside of the chamber. During a test, stress and strain data were automatically and periodically sampled and recorded by a computerized data acquisition system that is tied directly into the testing equipment. After each test had been performed, all test data is graphed, tabulated, and analyzed by computer.

3.0 RESULTS

Sample stress-strain curves produced for this work are shown in Fig. 1 through 6. Results of the tests performed are presented in Tables 1 to 4. Data is catagorized by stiffness (Table 1), strength (Table 2), Poisson's ratio (Table 3), and shear modulus (Table 4). Each table is then sub-divided according to laminate lay-up and test temperature. The data is plotted as a function of temperature in Figs. 7

through 21, and the coefficients of a least-squares fit of the data are presented in Tables 5 and 6.

3.1 Stress-Strain Curves

The data presented in Figs. 1 and 2 shows that stress-strain behavior is nearly linear for both the 0° and 90°-material at all test temperatures. The principal moduli increase at both 116K (-250°) and 394K (+250°F), with the larger increase occurring at the lower test temperature. In all cases, very little nonlinear behavior is noted prior to failure. The 0°-material does exhibit a stiffening behavior at high strains for room and elevated temperature [3].

Significant nonlinear behavior is exhibited in the stress-strain curves at room and elevated temperatures for the other laminates tested (Figs. 3-6). All four sets of stress-strain behavior ($[45]_8$, $[+30_2/-30_2]_s$, $[+45_2/-45_2]_s$, and $[+60_2/-60_2]_s$) show similar trends. At 116K (-250°F) the stress-strain curve is essentially linear. As the test temperature is increased, the elastic modulus decreases and the degree of nonlinearity increases. In all cases, the largest degree of nonlinearity is exhibited at the high test temperature. This behavior is as expected in view of the known influence of temperature on the response of the epoxy matrix material. The nonlinearity is more pronounced in the laminates whose behavior is more dominated by matrix properties. The nonlinearity is not evident in the $[90]_8$ laminate because of the low failure strain.

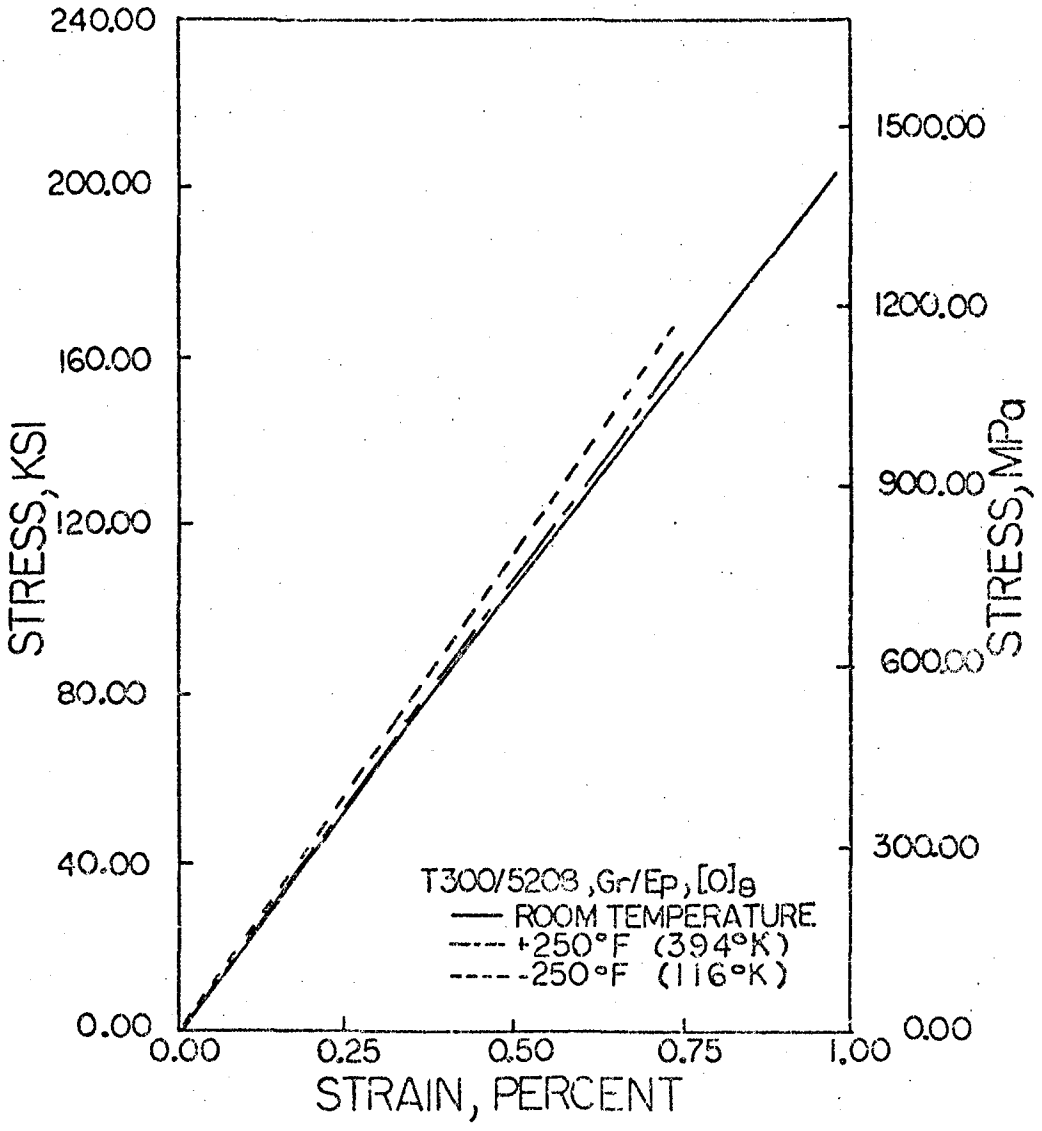

Fig. 1. Stress-Strain Curves as a Function of Temperature for the $[0]_8$ Laminate.

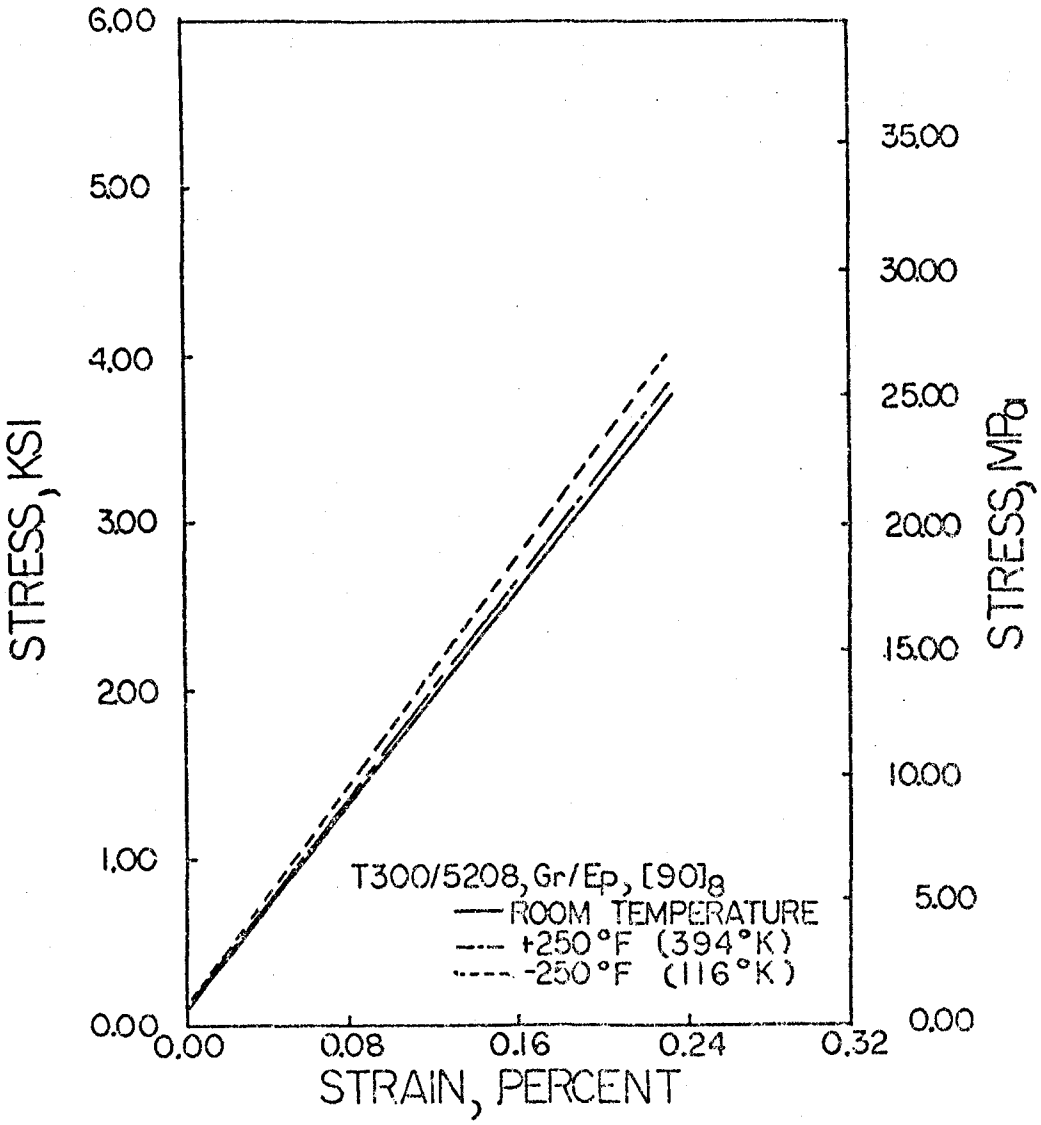

Fig. 2. Stress-Strain Curves as a Function of Temperature for the $[90]_8$ Laminate.

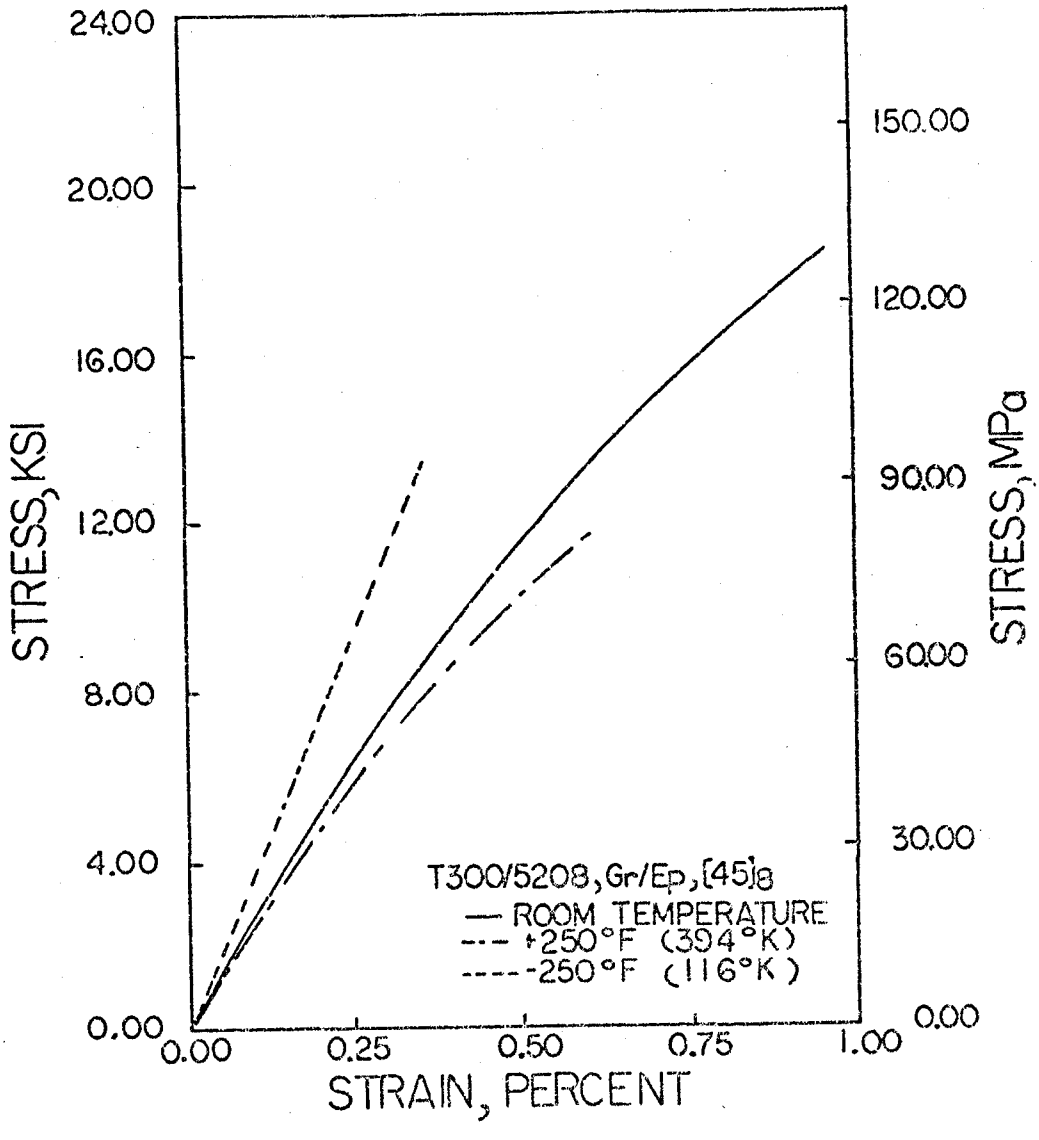

Fig. 3. Stress-Strain Curves as a Function of Temperature for the $[45]_8$ Laminate.

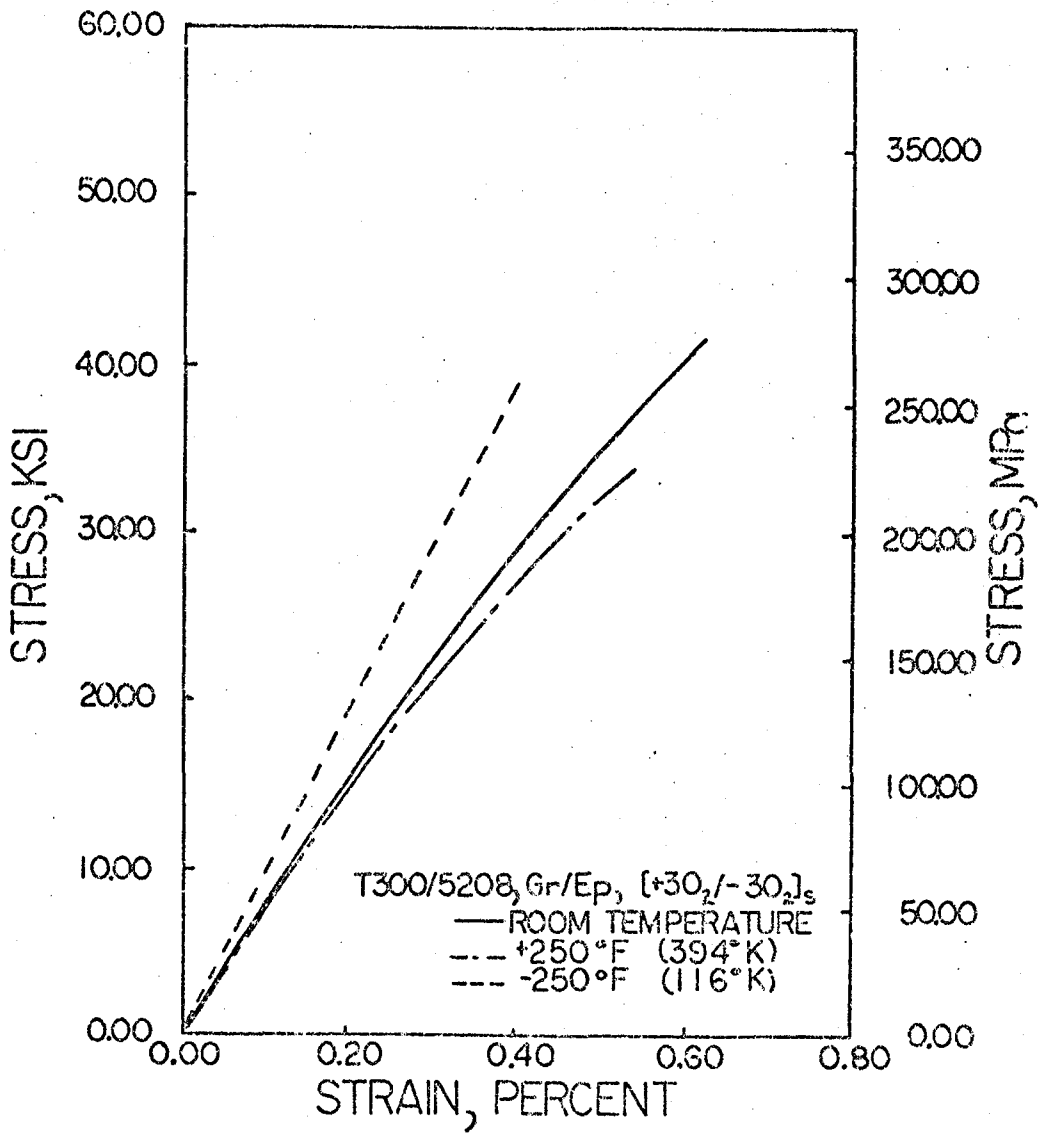

Fig. 4. Stress-Strain Curves as a Function of Temperature for the $[+30_2/-30_2]_s$ Laminate.

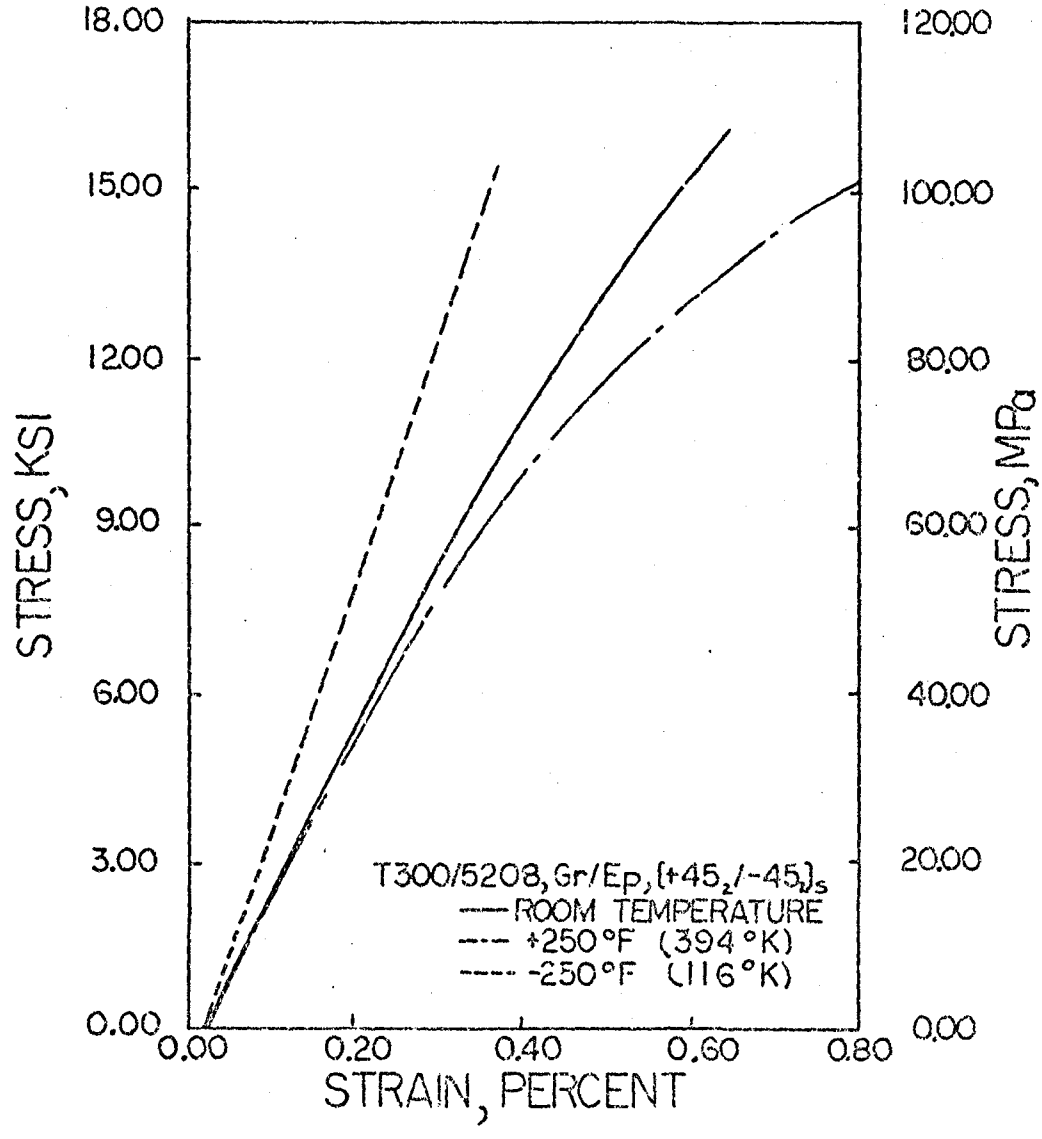

Fig. 5. Stress-Strain Curves as a Function of Temperature for the $[+45_2/-45_2]_s$ Laminate.

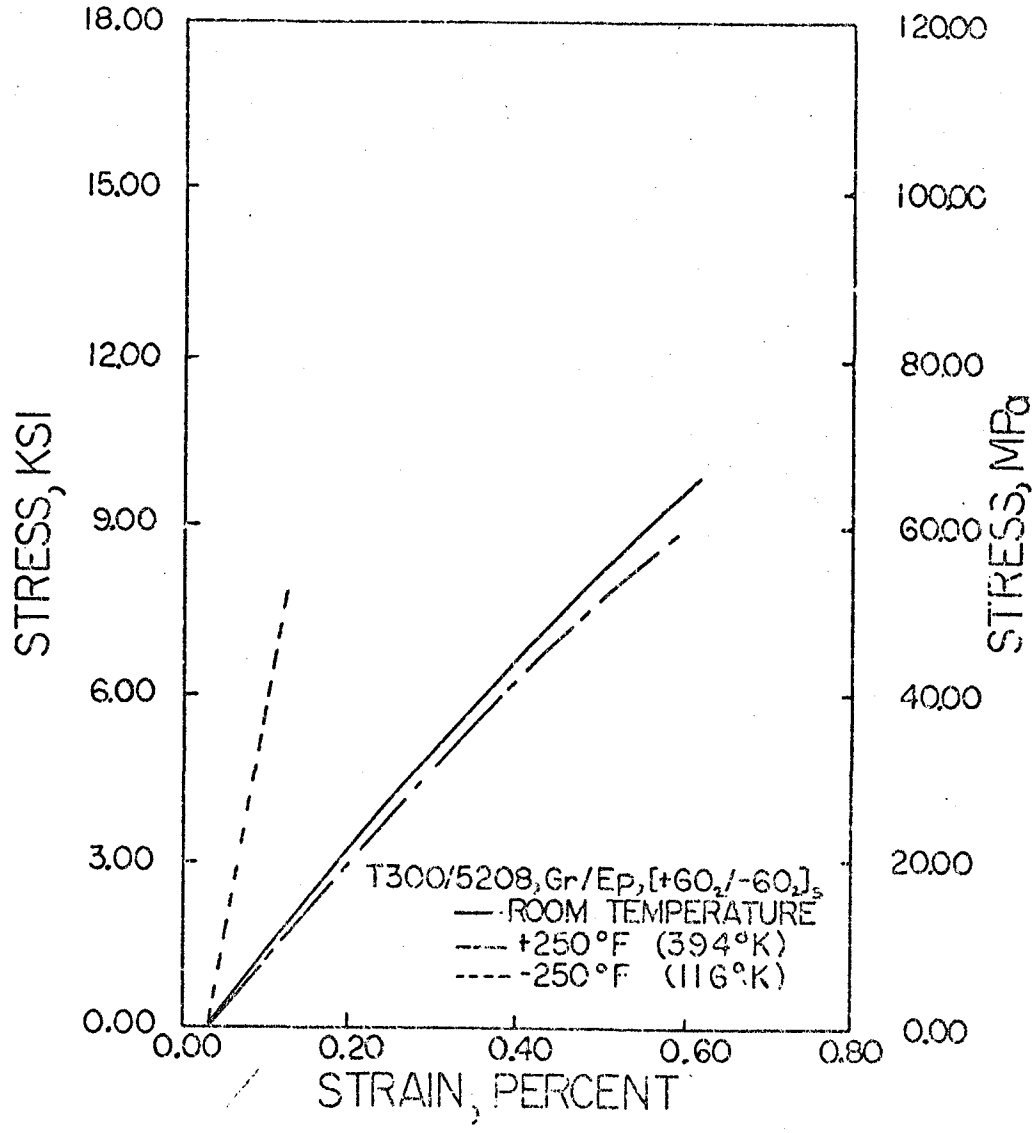

Fig. 6. Stress-Strain Curves as a Function of Temperature for the $[+60_2/-60_2]_s$ Laminate.

3.2 Elastic Properties

0°-laminate: E_1. The experimental results for the elastic modulus, E_1, are plotted as a function of temperature in Fig. 7. Moduli values are presented in Table 1 and the coefficients of a second-order curve fit are given in Table 5. The modulus is 6 to 7 percent higher at both elevated and low temperatures, as compared to that measured at room temperature. Since fiber properties are independent of temperature (over this range), the temperature dependence observed here is a function of the changing matrix properties, fiber waviness, and residual stresses [4]. The higher modulus at the elevated temperature is believed to be due primarily to reduced residual stresses which result in lower matrix stresses. Lower stresses in the matrix and straighter fibers should result in a higher modulus of the composite due to the absence of nonlinear matrix behavior [5-9]. The higher modulus at the lower temperature is a result of an increase in the stiffness of the matrix material. Apparently, the matrix is so stiff at low temperatures that its effect on the modulus of the composite overrides the effect of residual stresses.

90°-laminate: E_2. The results for the transverse modulus E_2, (Fig. 8, Tables 1 and 5) indicate that there is a 30 percent increase in the transverse modulus at the low temperature compared to the room temperature value. This indicates that the epoxy matrix material is much stiffer at the lower temperature. Epoxies are known to exhibit this type of behavior at low temperatures. In contrast to the low temperature results, increasing the temperature above room temperature has much less influence on the transverse modulus. Since increasing the test temperature acts to relieve residual stresses, we may conclude that

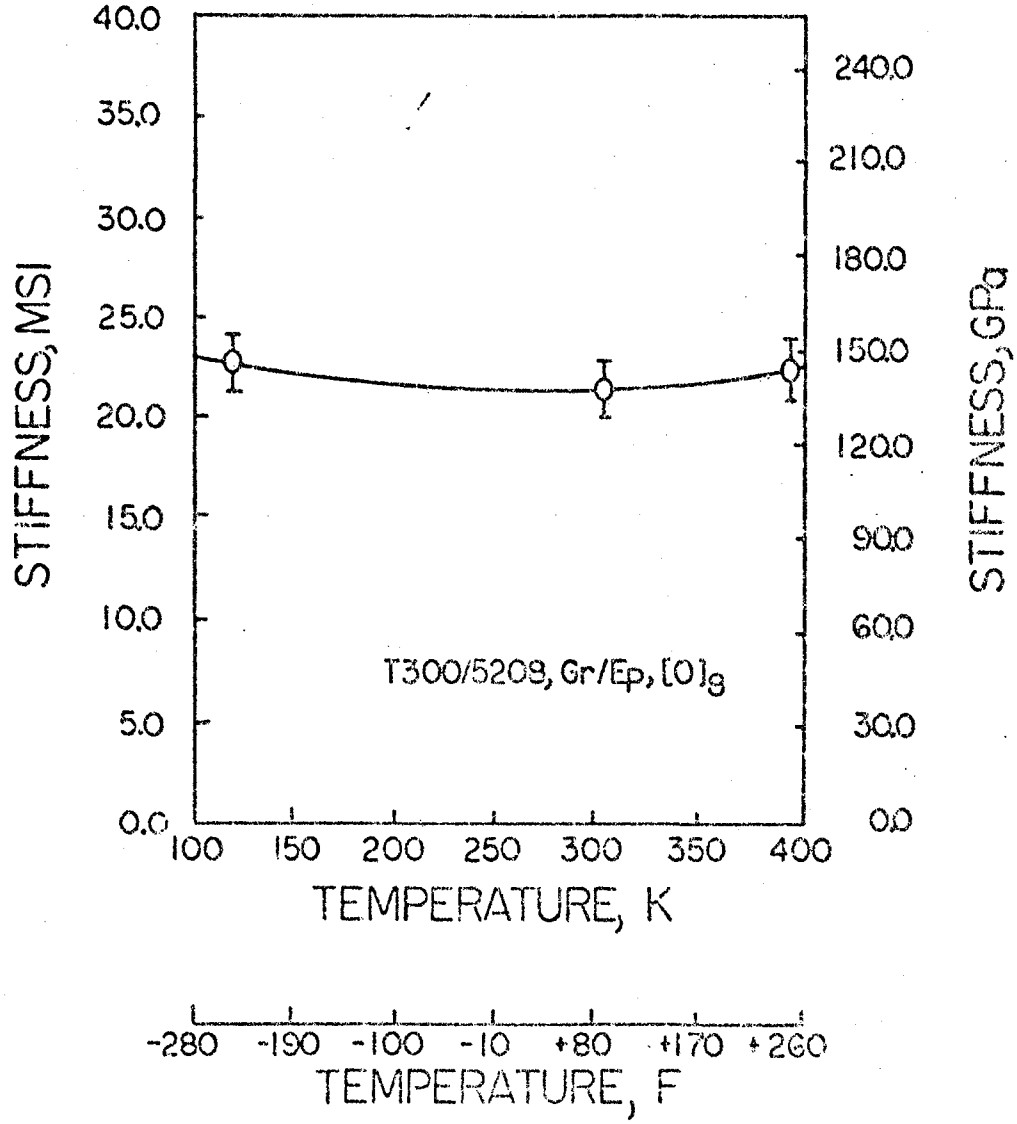

Fig. 7. Modulus of Elasticity, E_1, Versus Temperature.

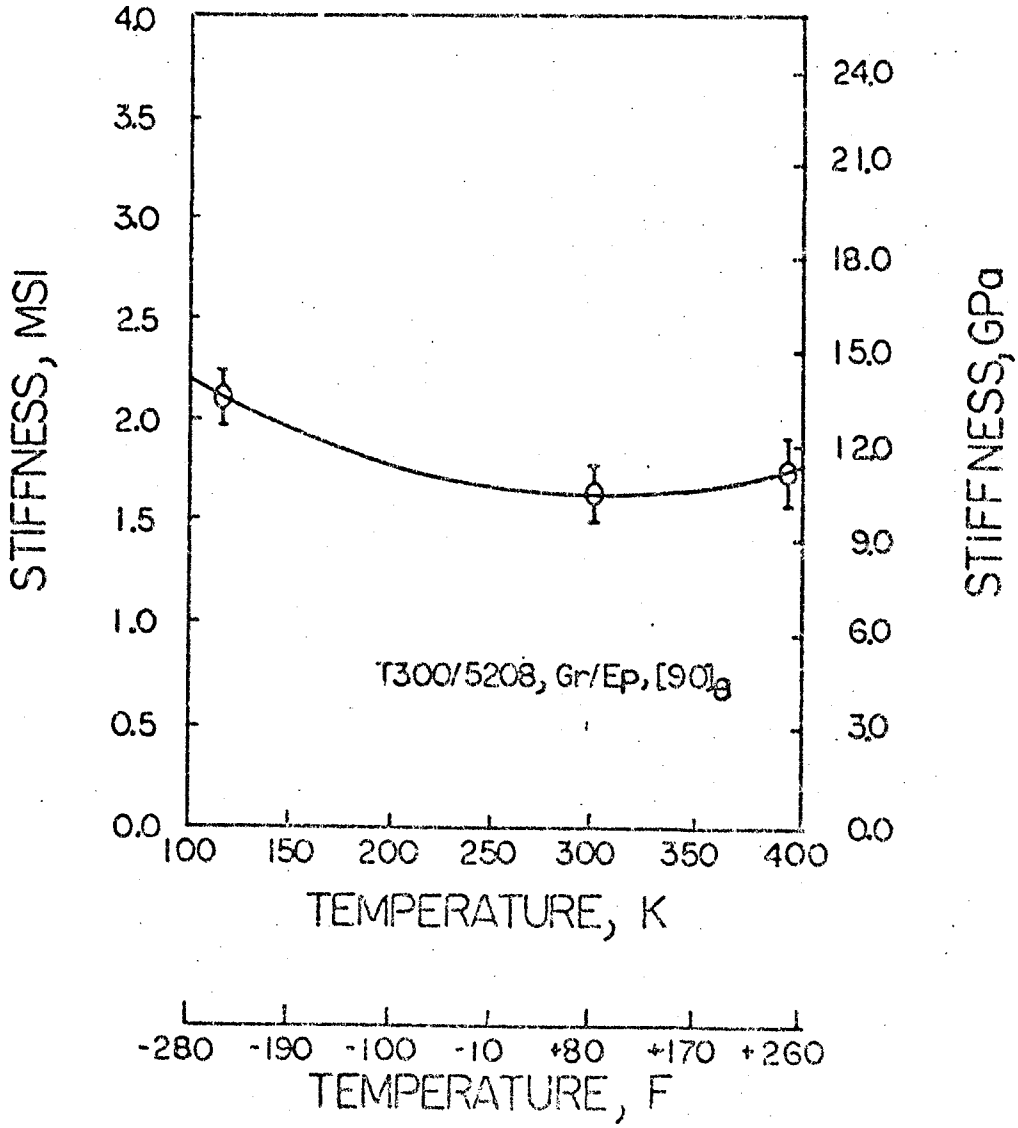

Fig. 8. Modulus of Elasticity, E_2, Versus Temperature.

residual stresses do not play as large a role in affecting transverse modulus as compared to their influence in the fiber direction. This is consistent with the much lower influence of fiber waviness on the transverse stiffness.

45°-laminate: G_{12}. This laminate was chosen as the best specimen for determination of the shear modulus, G_{12}, based upon the findings in reference [2].. Average results for the shear modulus, G_{12}, are plotted in Fig. 9 and values for modulus and a second-order fit are given in Tables 1, 4, and 5. The results were obtained using a 45-unidirectional off-axis specimen and the following standard relationship [10].

$$G_{12} = \left[\frac{4}{E_x} - \frac{1}{E_1} - \frac{1}{E_2} + \frac{2\nu_{12}}{E_1} \right]^{-1}$$

where E_x is the measured axial modulus of the 45°-specimen and the other quantities correspond to properties in the material principal coordinate system. The results indicate that a second-order curve fit provides an excellent correlation of the temperature dependence of G_{12}. The higher value at the low temperature is consistent with the temperature dependent response of matrix dominated properties.

The variation of the axial modulus, E_x, of the 45°-laminate with temperature is shown in Fig. 10 and values are given in Tables 1 and 6. Comparison between experimental and theoretical values (Table 1) indicates excellent agreement at room and elevated temperatures, but less than stisfactory agreement at the low temperature.

Poisson's ratio: ν_{12}. The temperature dependence of ν_{12}, (Fig. 11) is essentially linear, decreasing with increasing temperature. The

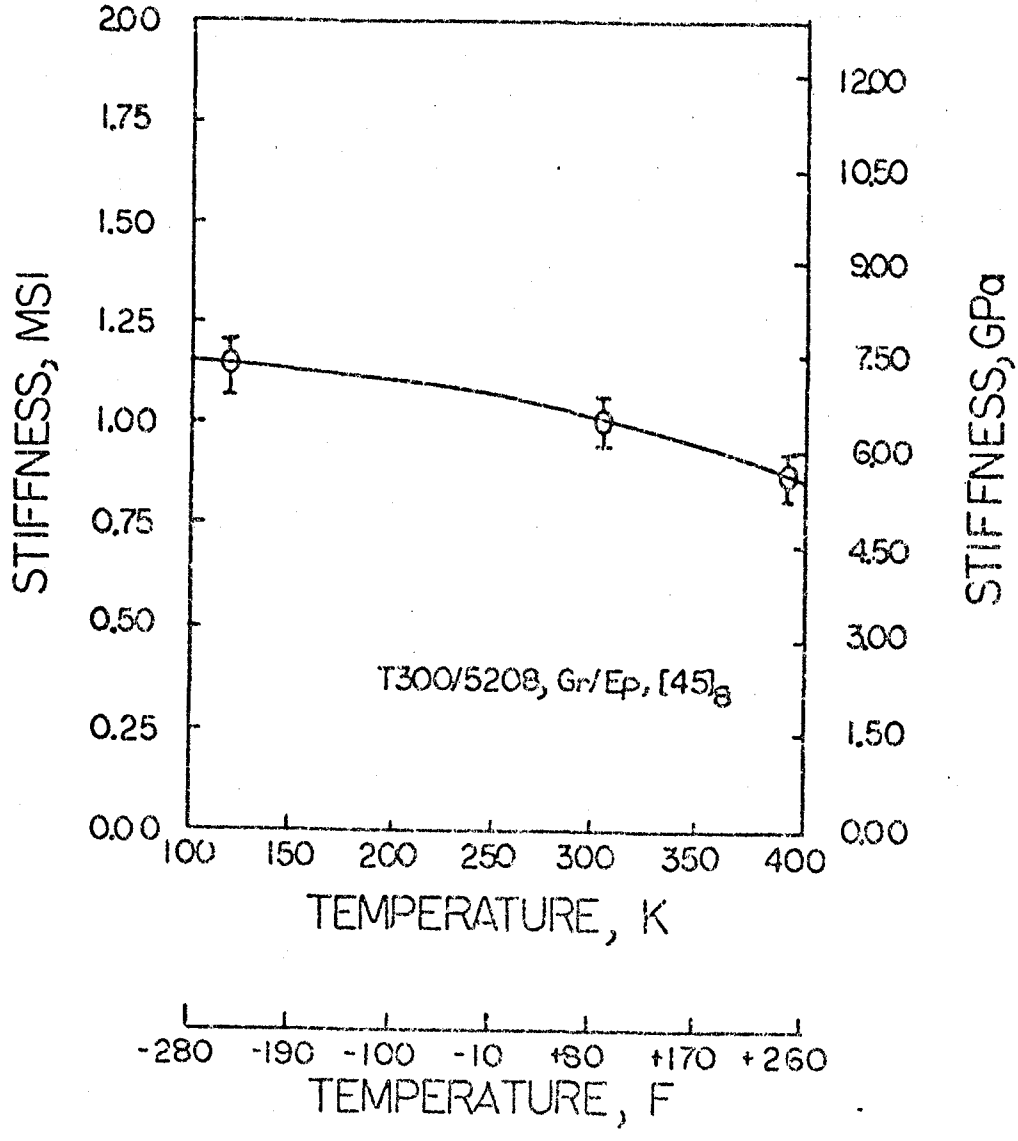

Fig. 9. Shear Modulus, G_{12}, Versus Temperature.

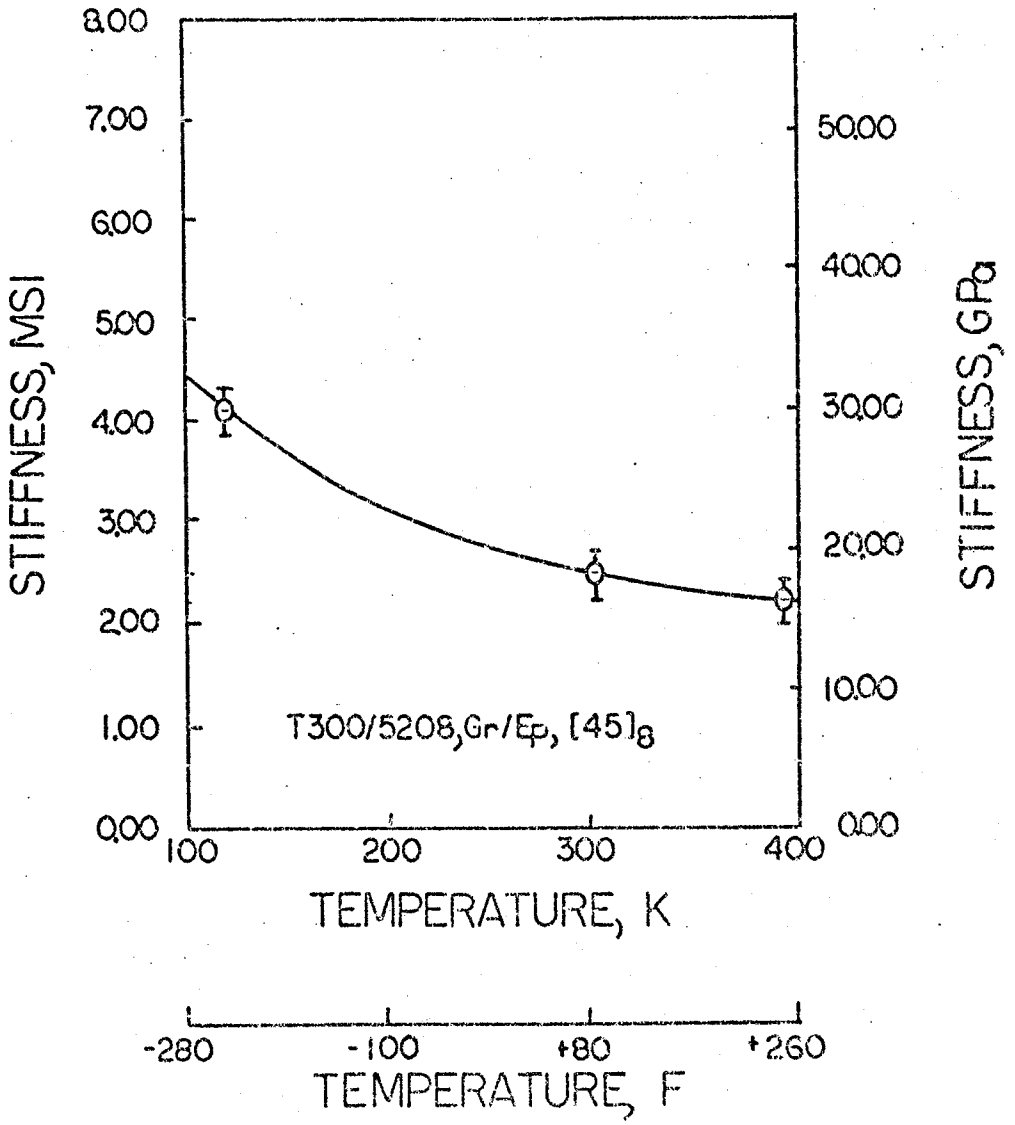

E_x

Fig. 10. Axial Modulus of the $[45]_8$ Laminate Versus Temperature.

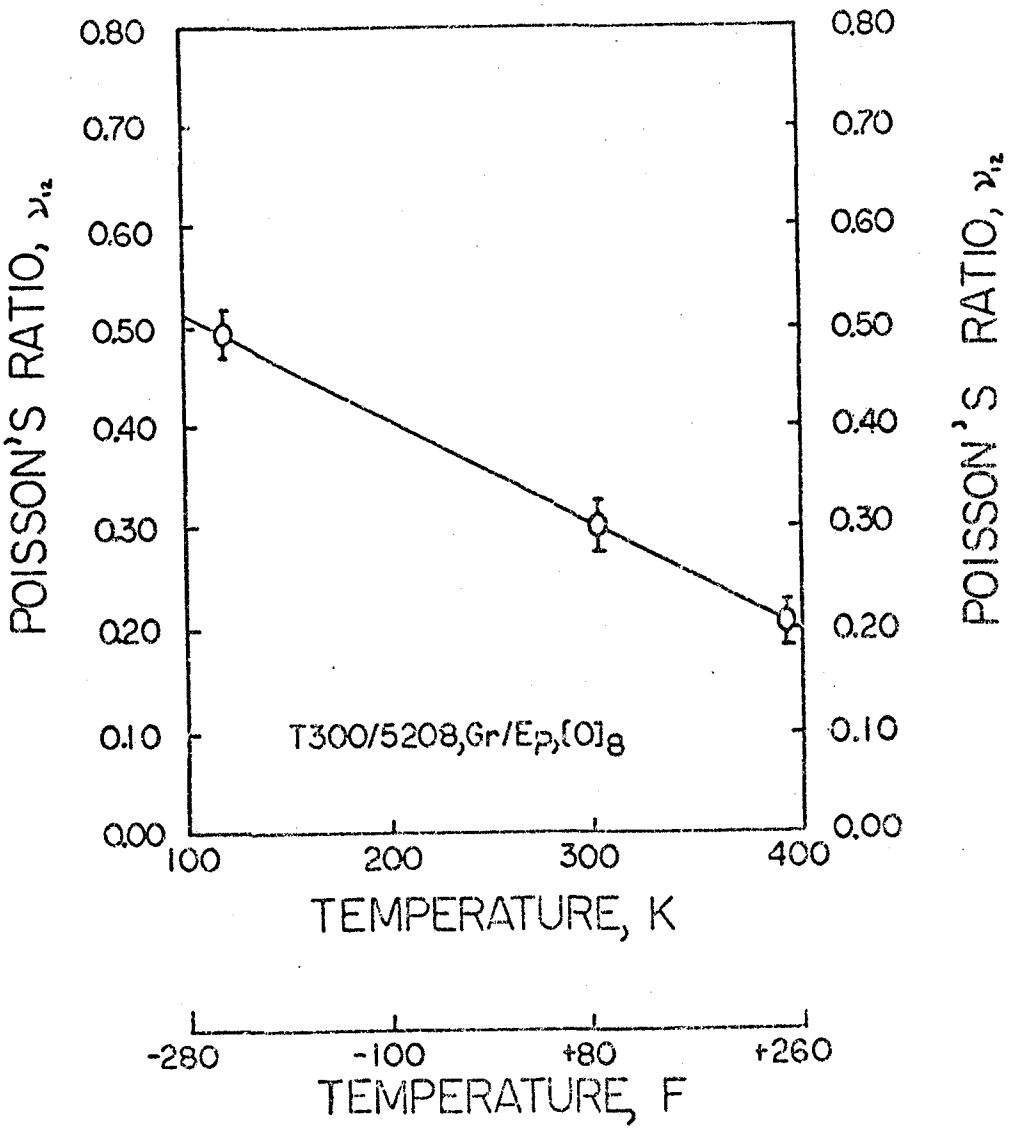

Fig. 11. Poisson's Ratio, ν_{12}, Versus Temperature.

higher Poisson's ratio at the low temperature is somewhat surprising in view of the elastic symmetry condition:

$$\nu_{12} = \nu_{21} \cdot \frac{E_1}{E_2}$$

The modulus ratio, E_1/E_2, is smaller at the low temperature compared to the room temperature ratio. Thus a higher ν_{12} at the low temperature should be accompanied by a significantly higher ν_{21} at the low temperature. While this trend was evident from the experimental results, the values did not correspond to satisfaction to the E•ν relationship. In fact, the measured value of ν_{21} was much too high. Accurate measurement of the small strains involved is very difficult due to errors introduced by the transverse sensitivity of the strain gages. In the case of 90°-material, transverse sensitivity became prohibitively large compared to the small strains that were measured.

Angle-ply laminates. Results for the effect of temperature on the modulus of the angle-ply laminates tested are shown in Figs. 12-14, and Tables 1 and 6. As the temperature increases, the modulus decreases for all laminates. The decrease in modulus with temperature increase is also illustrated in the stress-strain curves for these laminates (Figs. 3 to 6). As discussed in previous sections, at low temperatures the epoxy matrix becomes stiffer resulting in increased laminate stiffness. The stress-strain curves exhibit increased nonlinearity with increasing temperature. This results in decreased overall stiffness in the laminate. It should be noted here that reduced residual stresses (at higher temperature) are not expected to influence the stiffness of these laminates nearly as much as it influences the stiffness of unidi-

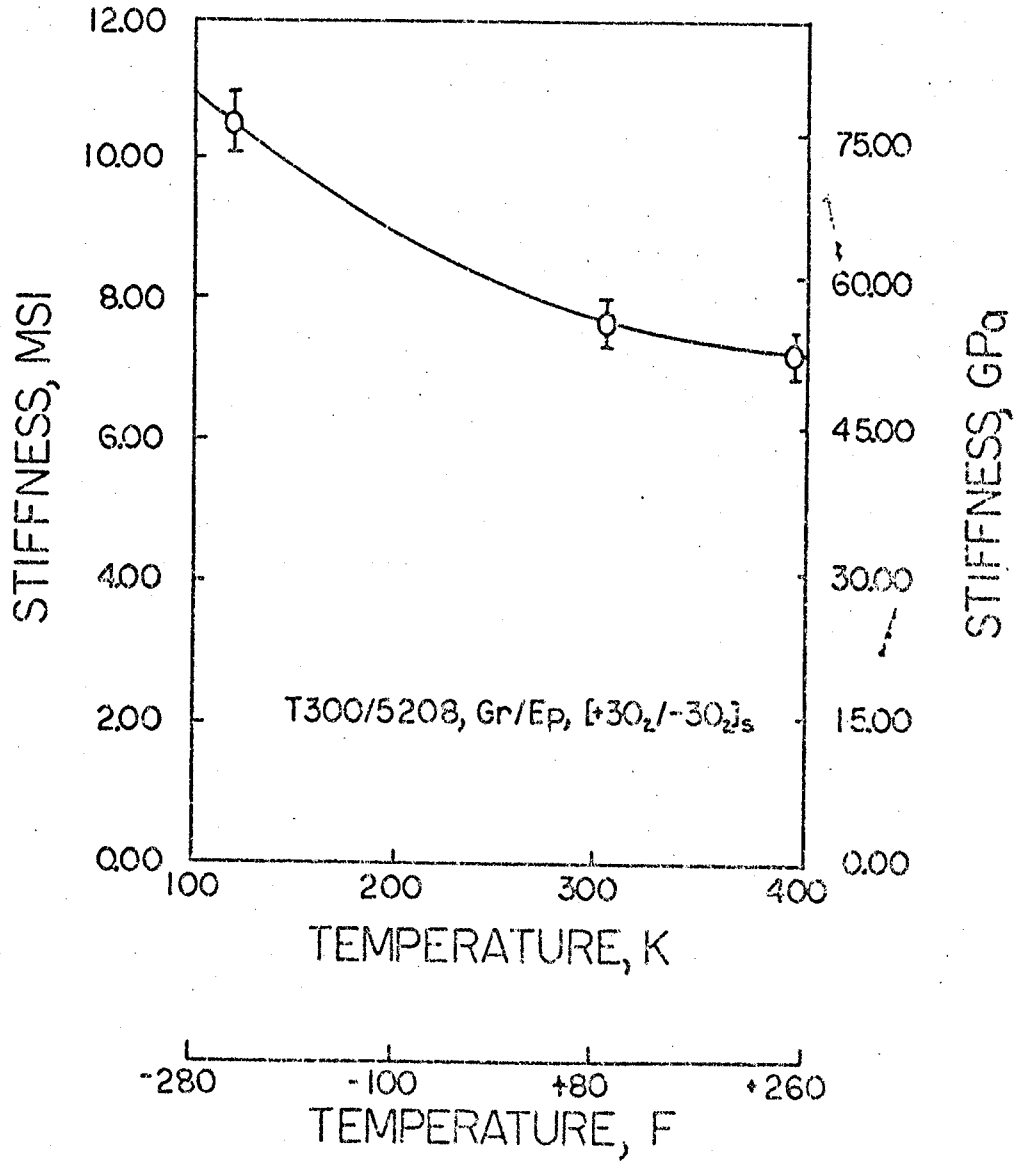

Fig. 12. Axial Modulus of the $[+30_2/-30_2]_s$ Laminate Versus Temperature.

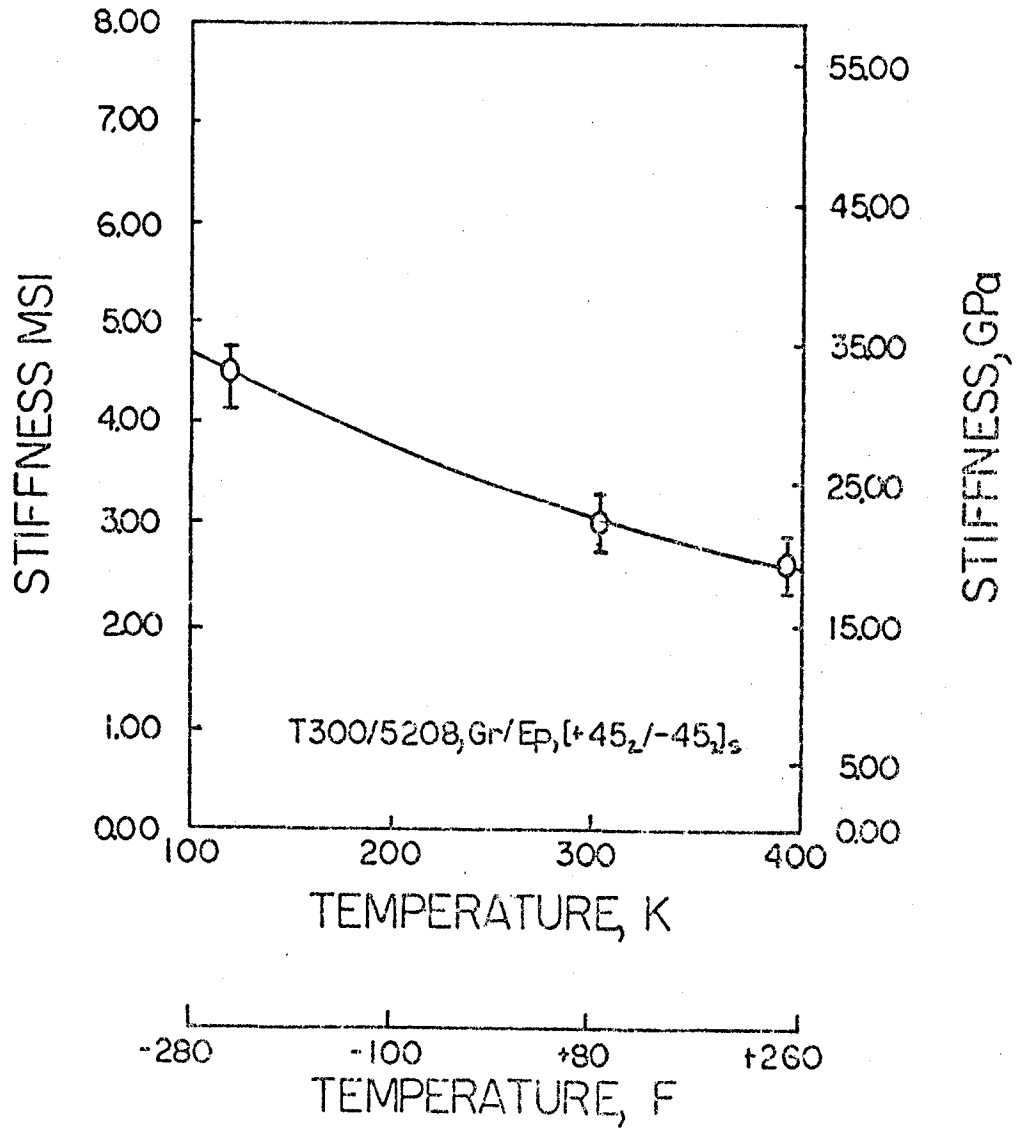

Fig. 13. Axial Modulus of the $[+45_2/-45_2]_s$ Laminate Versus Temperature.

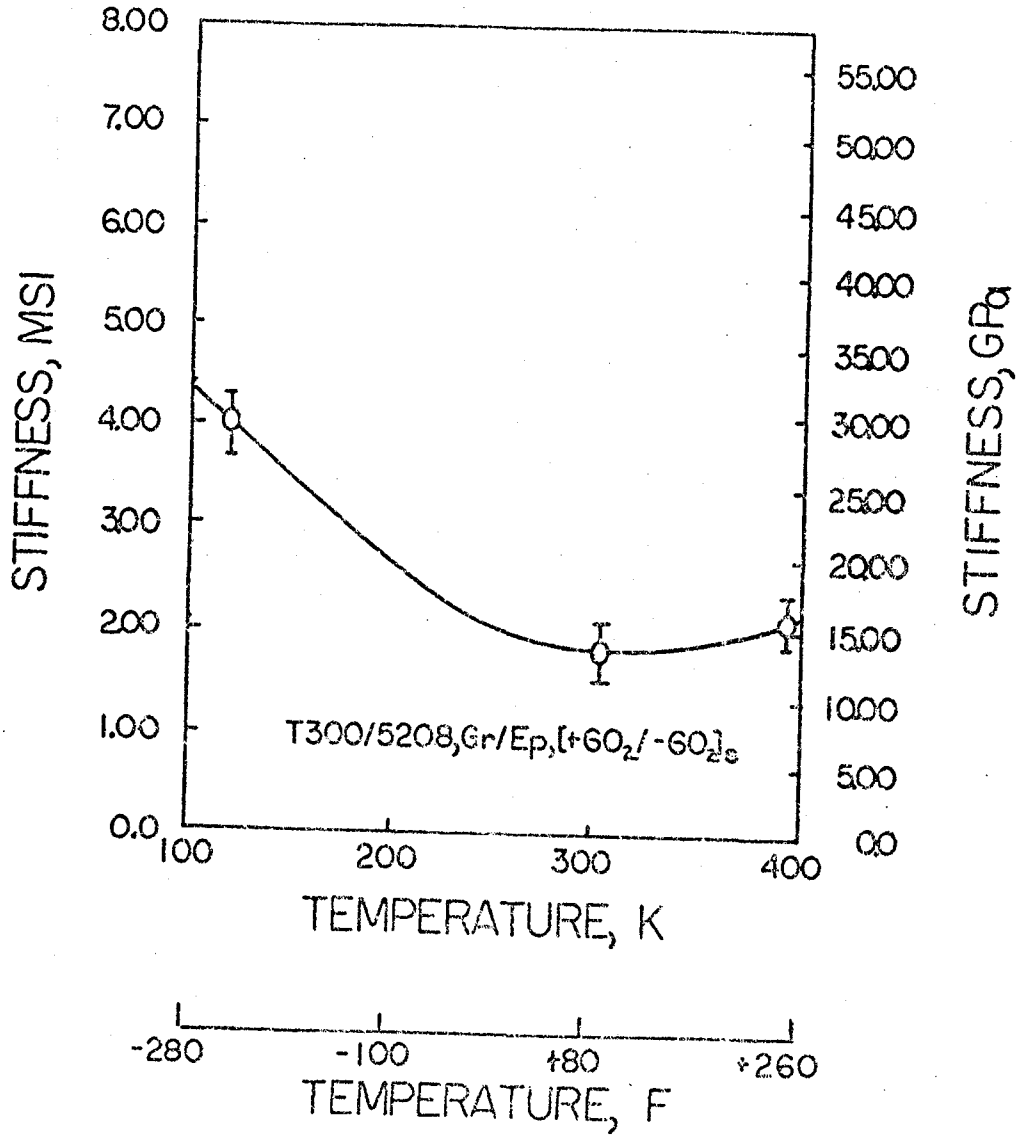

Fig. 14. Axial Modulus of the $[+60_2/-60_2]_s$ Laminate Versus Temperature.

rectional material in the fiber direction. As with the 45-laminate, comparison between experimental and theoretical values (Table 1) indicates excellent agreement at room and elevated temperatures, but less than satisfactory agreement at the low temperature.

3.3 Strength Properties

0°-laminate: X_T. Results for the temperature dependence of 0°-laminate strength, including the type of failure mode noted, are shown in Figs. 15 and 16. It is observed that the strength increases nearly linearly with increasing temperature. These results are apparently due to changing matrix properties and residual stresses. At the lower temperature, the matrix is brittle and stiff, resulting in higher residual stresses and less efficient load transfer in regions of stress concentration such as at fiber breaks. The reverse is true at elevated temperatures.

The type of failure mode observed after the tensile tests of $[0]_8$ laminates is indicated in Fig. 12. The room temperature and high temperature tests both exhibit a "shatter-type" failure mode. When the composite test specimen fails in this mode, the specimen splits parallel to the fibers into many small pieces. Very little of the original specimen is left intact. This phenomenom appears to be more severe with increasing temperature. On the other hand, low temperature tests exhibit a "transverse-break" failure mode. Instead of splitting, the composite specimen fails by a single jagged break across its width. This is further evidence that the matrix material becomes more brittle at low test temperatures. These results may be an indication that the fiber/matrix bond is stronger at the low temperature. This could be the

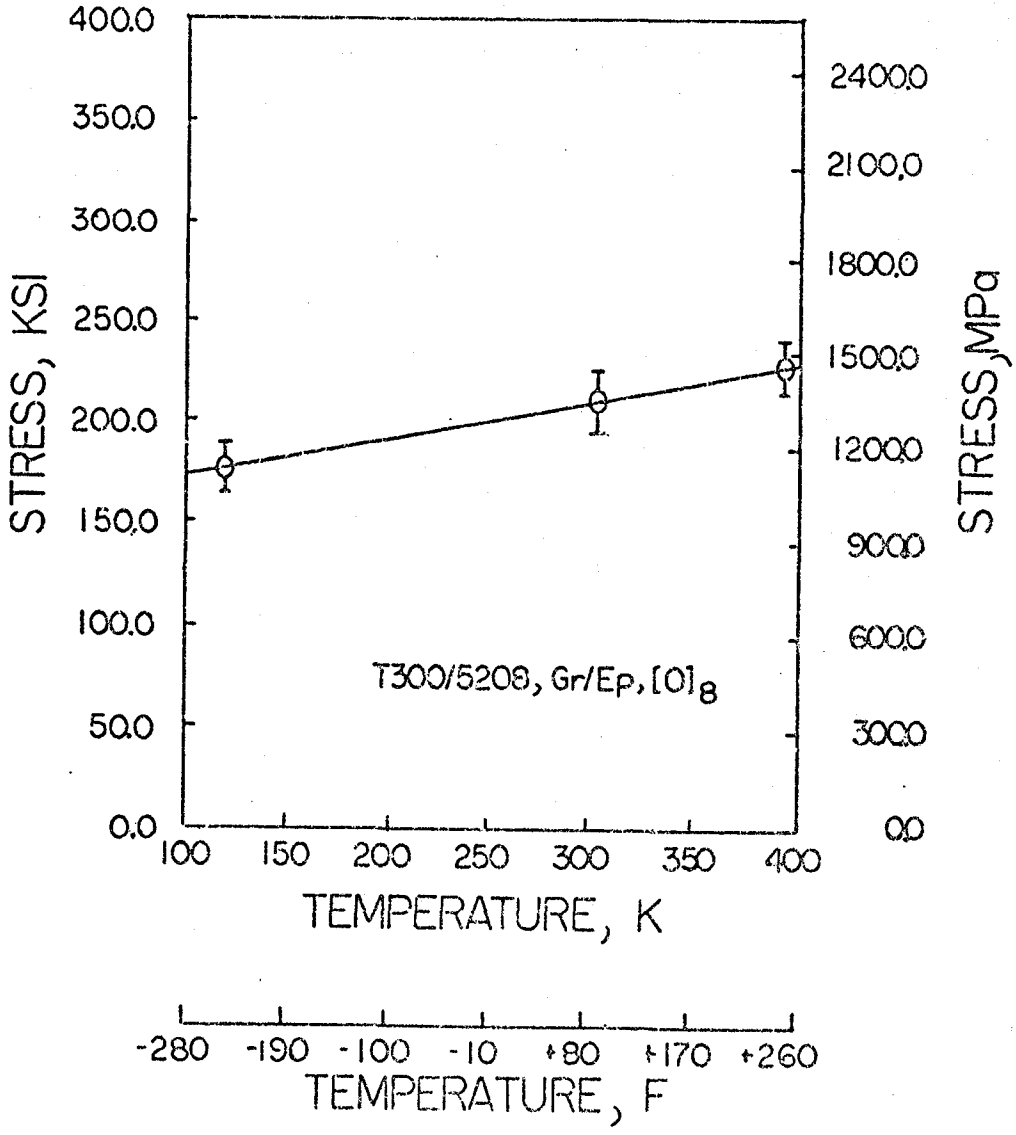

Fig. 15. Ultimate Strength, X_T, Versus Temperature.

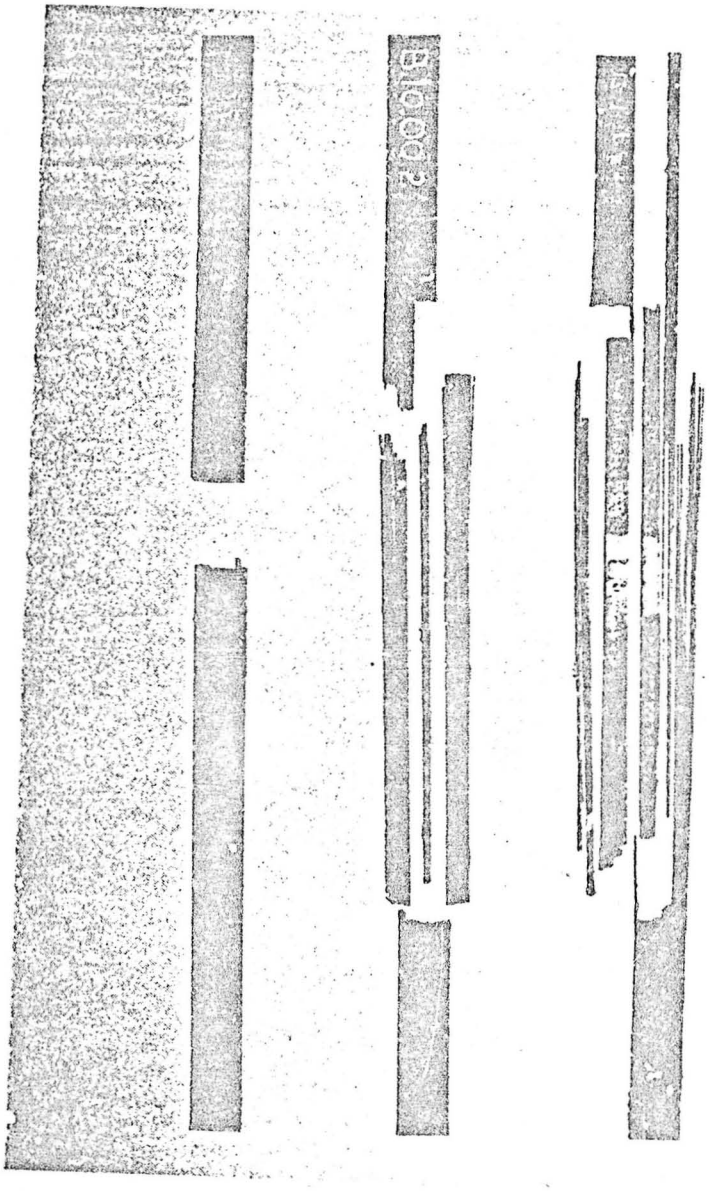

Room Temperature (294K)

-250°F (116K)

+250°F (394K)

Fig. 16. Failure Modes of the $[0]_8$ Laminate as a Function of Temperature.

result of a much tighter "shrink-fit" due to the higher residual stresses in the brittle matrix material.

90°-laminate: Y_T. The results in Fig. 17 indicate that the transverse strength is not influenced strongly by temperature. As indicated in the figure, there is considerable scatter in the data at all three test temperatures. This is typical of tests on 90°-material.

45°-laminate. The temperature dependence of the strength of this laminate is shown in Fig. 18. Clearly, there is significant variation in strength depending upon the temperature. This laminate fails in a mixed mode of inplane shear and transverse tension. Thus it is not a good specimen for determination of fundamental properties, but rather useful for correlation of theory and experiment for failure under biaxial loading. Such comparison will not be made here. The results are presented for completeness. As mentioned previously, the specimen was chosen for measurement of shear modulus, not shear strength.

Angle-ply laminates. Temperature dependent strength results for the angle-ply laminates are presented in Figs. 19-21 and Tables 2 and 6. The data shows that laminate strength does not follow a consistent trend as a function of temperature. Obviously, these laminates are affected in different ways and to different degrees by the changes in the composite induced by temperature. A complex interaction occurs between the increasing stiffness of the matrix (with decreasing temperature), the increase in fiber-direction strength (with increasing temperature), and the effect of residual stresses that may or may not be relieved by combinations of the above properties. All these interactions make precise strength predictions difficult for laminates.

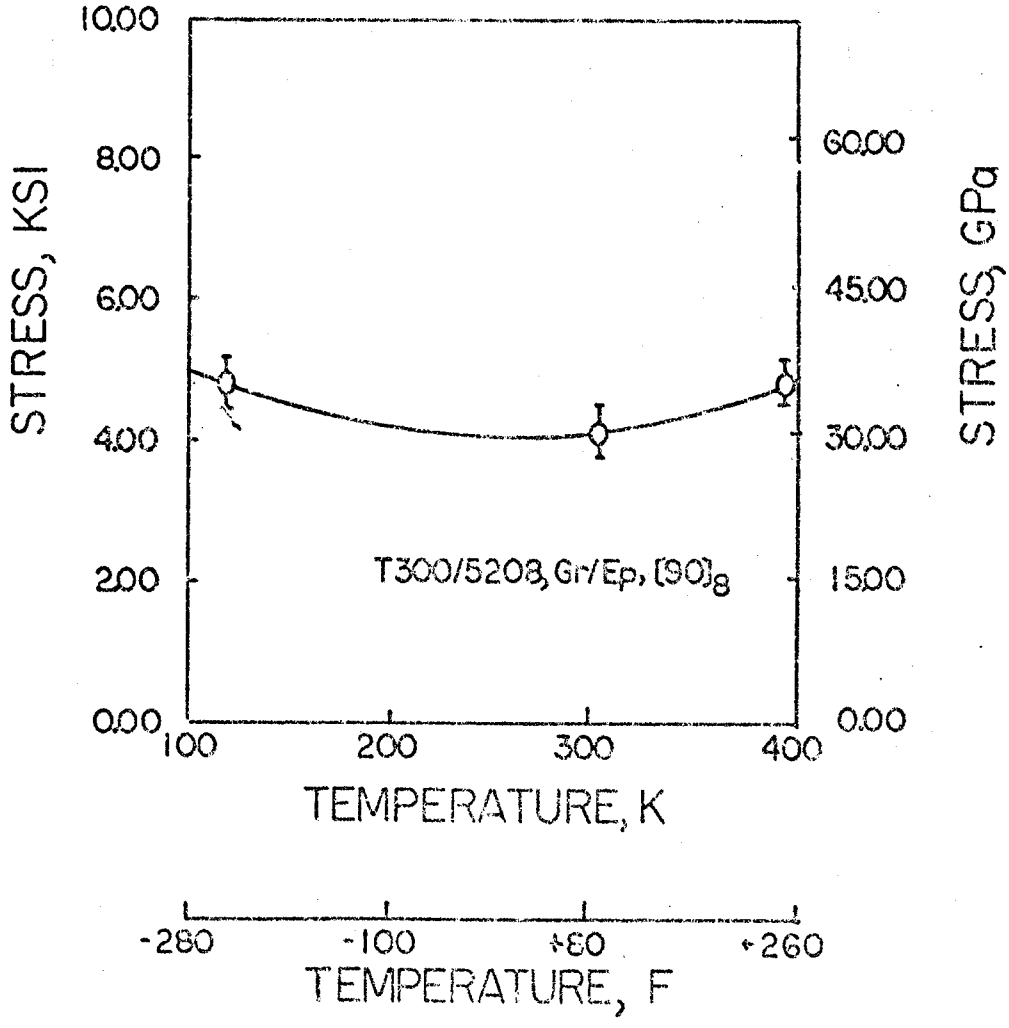

Fig. 17. Ultimate Strength, Y_T, Versus Temperature.

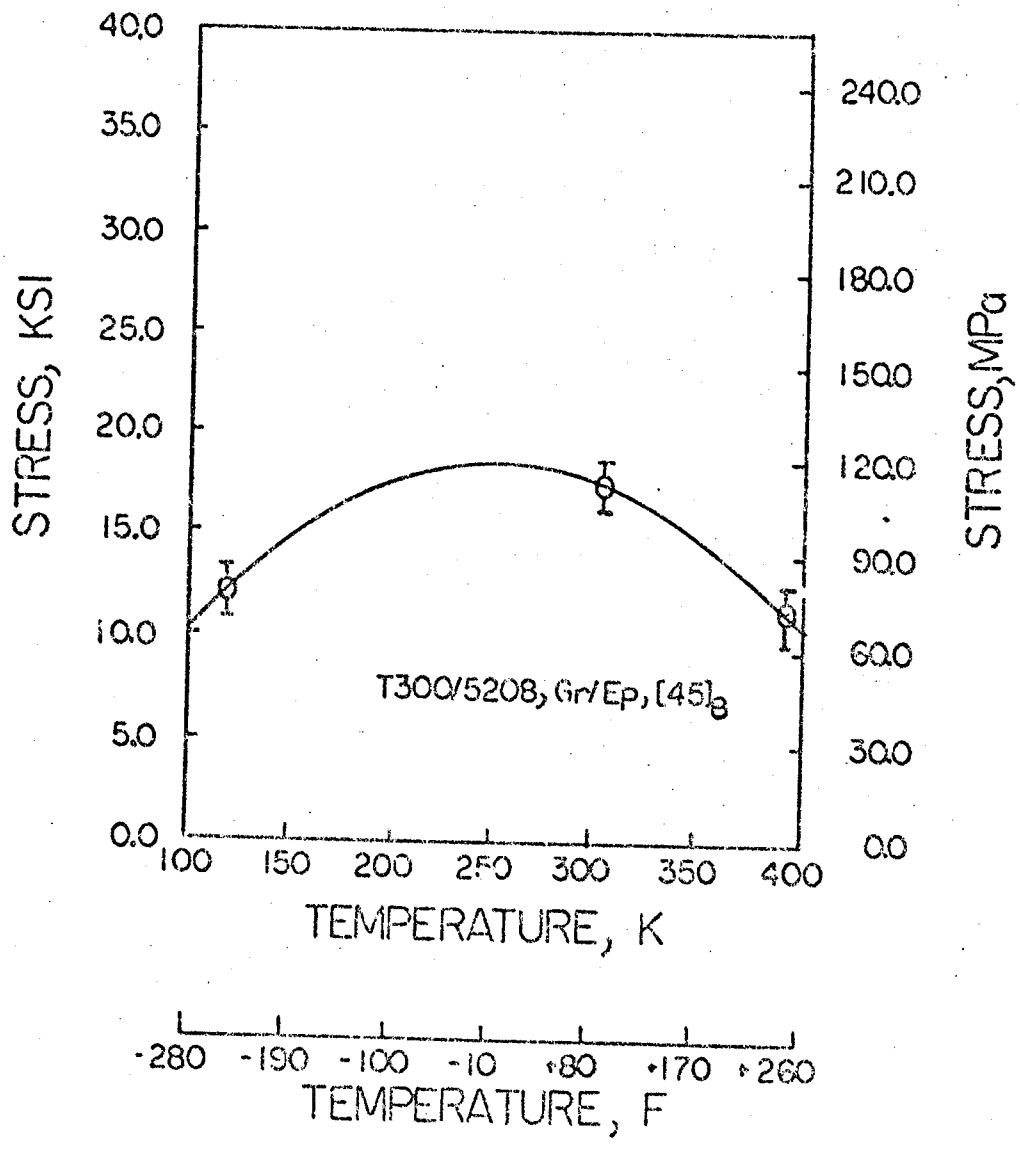

Fig. 18. Ultimate Strength of the $[45]_8$ Laminate Versus Temperature.

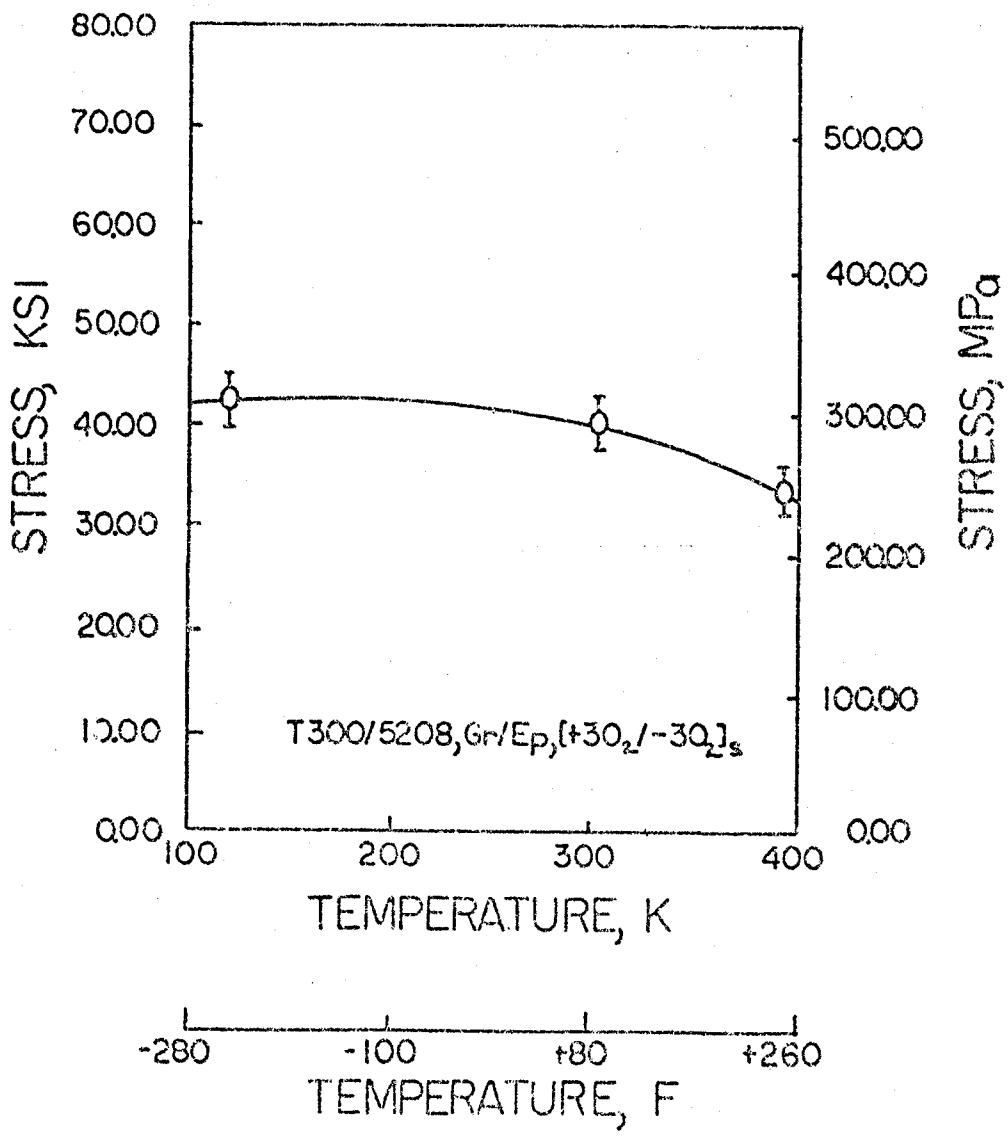

Fig. 19. Ultimate Strength of the $[+30_2/-30_2]_s$ Laminate Versus Temperature.

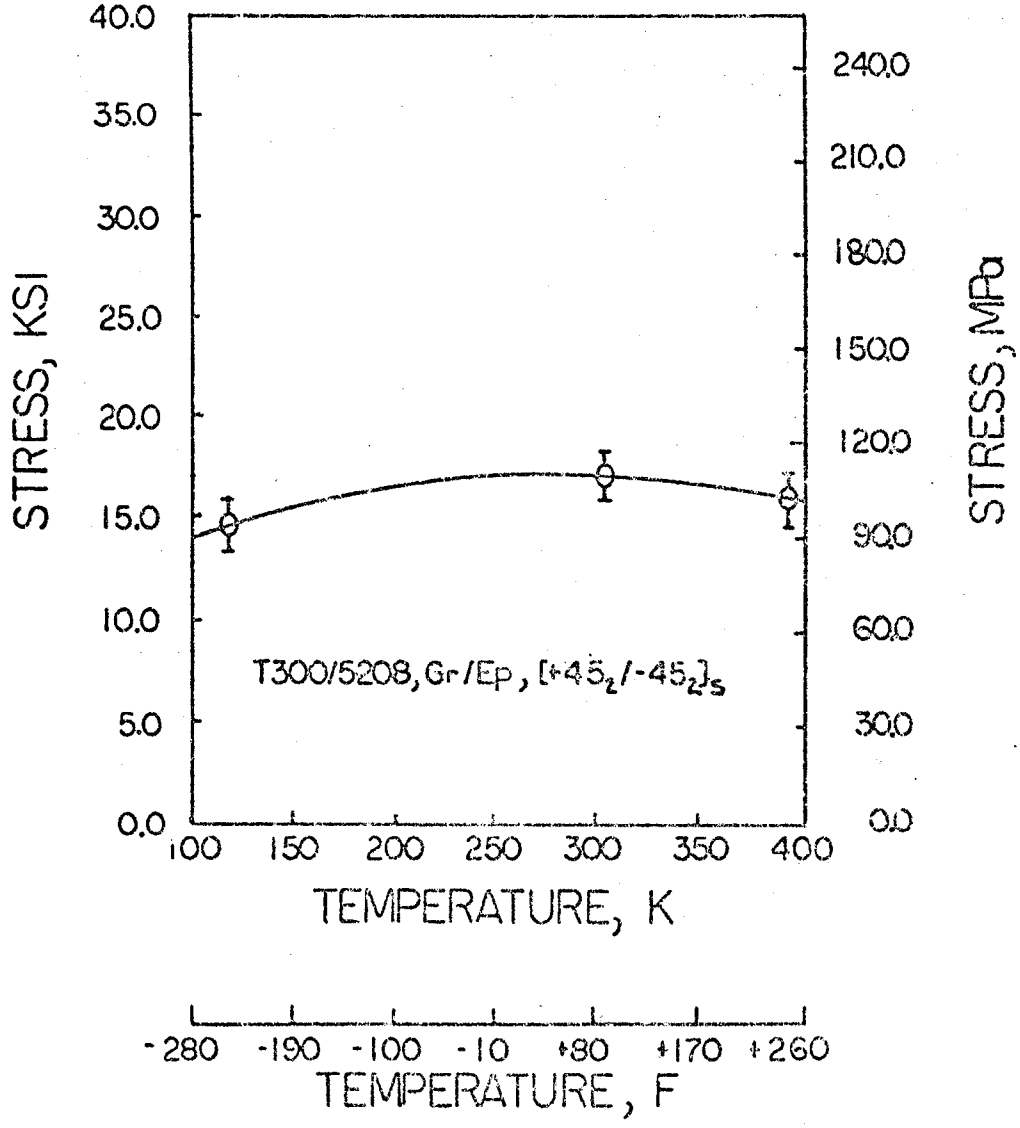

Fig. 20. Ultimate Strength of the $[+45_2/-45_2]_s$ Laminate Versus Temperature.

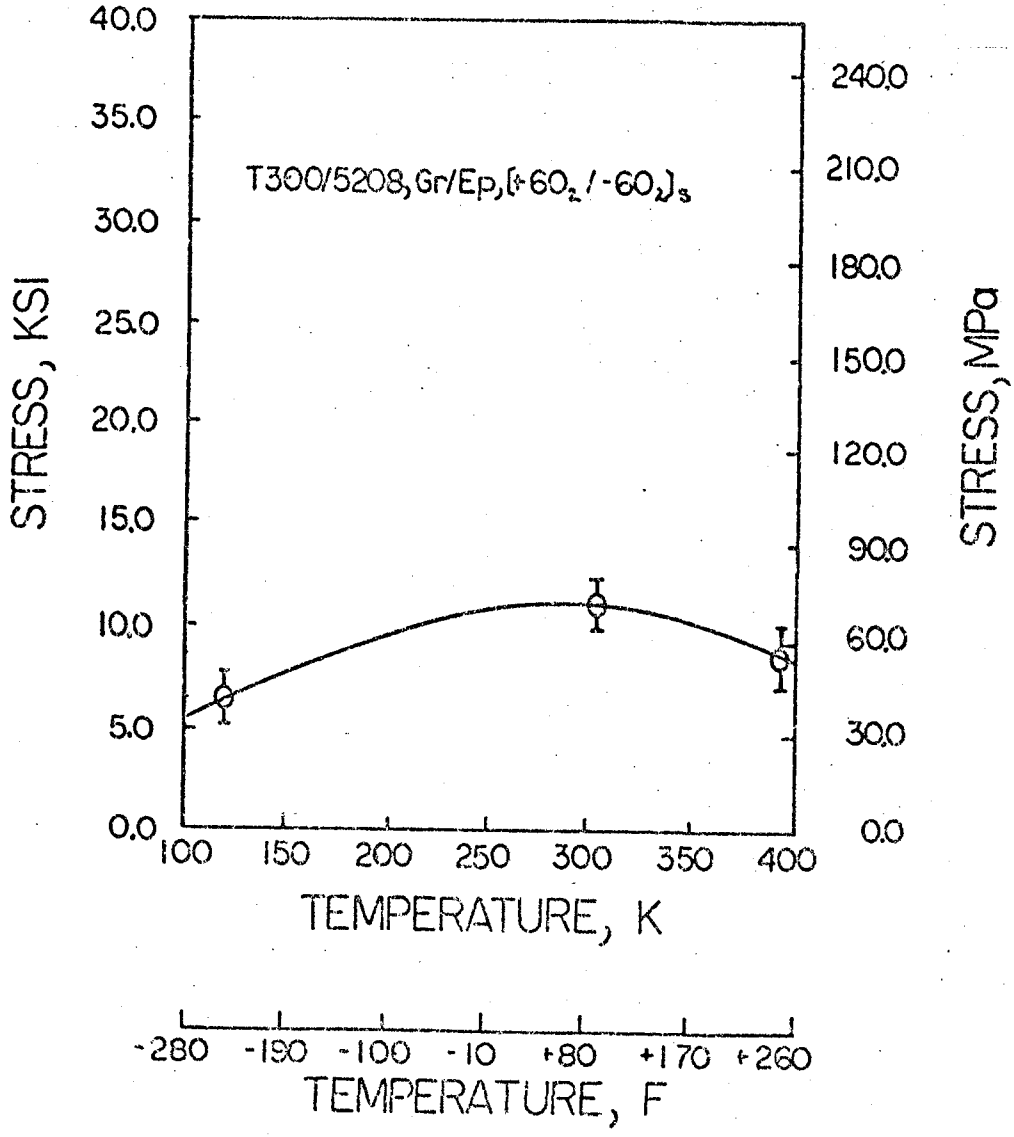

Fig. 21. Ultimate Strength of the $[+60_2/-60_2]_s$ Laminate Versus Temperature.

TABLE 1

Stiffness (E_x) Versus Temperature Data

Lay-up	116K (-250°F)	301K (R.T.)	394K (+250°F)
$[0]_8$:E_1	157.9GPa (22.90msi)	147.7 (21.42)	156.0 (22.62)
$[45]_8$	28.2 (4.089)	16.9 (2.452)	15.2 (2.211)
<THEORETICAL>*	20.3 (2.950)	16.9 (2.450)	15.2 (2.210)
$[90]_8$	14.5 (2.100)	11.1 (1.614)	11.7 (1.695)
$[+30_2/-30_2]_s$	70.4 (10.217)	52.2 (7.578)	50.3 (7.291)
<THEORETICAL>*	63.2 (9.160)	70.9 (8.420)	55.8 (8.090)
$[+45_2/-45_2]_s$	31.2 (4.523)	20.7 (2.997)	18.2 (2.638)
<THEORETICAL>*	27.0 (3.910)	23.8 (3.450)	20.3 (2.950)
$[+60_2/-60_2]_s$	27.6 (4.000)	12.5 (1.814)	14.6 (2.116)
<THEORETICAL>*	17.0 (2.470)	14.1 (2.050)	12.8 (1.860)

*Classical lamination theory

TABLE 2

Strength (σ_{ult}) Versus Temperature Data

Lay-up	116K (-250°F)	301K (R.T.)	394K (+250°F)
$[0]_8$:X_T	1,210MPa (175.7 ksi)	1,450 (209.7)	1,570 (228.0)
$[45]_8$	82.9 (12.02)	120.9 (17.54)	78.9 (11.45)
$[90]_8$:Y_T	33.2 (4.815)	28.3 (4.107)	32.6 (4.729)
$[+30_2/-30_2]_s$	294.1 (42.66)	276.5 (40.10)	227.9 (33.05)
$[+45_2/-45_2]_s$	101.9 (14.78)	112.5 (16.32)	104.4 (15.14)
$[+60_2/-60_2]_s$	45.2 (6.56)	74.3 (10.77)	59.0 (8.55)

TABLE 3

Poisson's Ratio (ν_{12}) versus Temperature Data

Lay-up	116K (-250°F)	301K (R.T.)	394K (+250°F)
$[0]_8$:ν_{12}	0.4922	0.2979	0.2098

TABLE 4

Shear Modulus (G_{12}) Versus Temperature Data

Lay-up	116K (-250°F)	301K (R.T.)	394K (+250°F)
$[45]_8$:G_{12}	7.85GPa (1.138msi)	6.94(1.007)	5.78 (0.8379)

TABLE 5

Coefficients for Elastic and Strength Temperature Dependence

$$P = C_0 + C_1 \cdot T + C_2 \cdot T^2$$

where P is the property of interest and T is in kelvin.

Property	C_0	C_1	C_2
E_1 (GPa)	0.1824×10^3	-0.2713×10^0	0.5184×10^{-3}
E_1 (msi)	0.2645×10^2	-0.3935×10^{-1}	0.7519×10^{-4}
E_2 (GPa)	0.1961×10^2	-0.5429×10^{-1}	0.8674×10^{-4}
E_2(msi)	0.2844×10^1	-0.7874×10^{-2}	0.1258×10^{-4}
ν_{12}	0.6092×10^0	-0.1021×10^{-2}	---
G_{12} (GPa)	0.7495×10^1	0.6599×10^{-2}	-0.2753×10^{-4}
G_{12} (msi)	0.1087×10^1	0.9571×10^{-3}	-0.3993×10^{-5}
X_T (MPa)	0.1060×10^4	0.1293×10^1	---
X_T (ksi)	0.1538×10^3	0.1875×10^0	---
Y_T (MPa)	0.4537×10^2	-0.1351×10^0	0.2608×10^{-3}
Y_T (ksi)	0.6580×10^1	-0.1960×10^{-1}	0.3782×10^{-4}

TABLE 6

Property	C_0	C_1	C_2
E_x, $[45]_8$ (GPa)	0.4069×10^2	-0.1257×10^0	0.1552×10^{-3}
E_x, $[45]_8$ (msi)	0.5901×10^1	-0.1823×10^{-1}	0.2251×10^{-4}
E_x, $[+30_2/-30_2]_s$ (GPa)	0.9143×10^2	-0.2140×10^0	0.2773×10^{-3}
E_x, $[+30_2/-30_2]_s$ (msi)	0.1326×10^2	-0.3103×10^{-1}	0.4021×10^{-4}
E_x, $[+45_2/-45_2]_s$ (GPa)	0.4158×10^2	-0.1023×10^0	0.1089×10^{-3}
E_x, $[+45_2/-45_2]_s$ (msi)	0.6031×10^1	-0.1483×10^{-1}	0.1579×10^{-4}
E_x, $[+60_2/-60_2]_s$ (GPa)	0.5008×10^2	-0.2373×10^0	0.3734×10^{-3}
E_x, $[+60_2/-60_2]_s$ (msi)	0.7263×10^1	-0.3441×10^{-1}	0.5416×10^{-4}
σ_{ult}, $[45]_8$, (MPa)	-0.2353×10^2	0.1191×10^1	-0.2364×10^{-2}
σ_{ult}, $[45]_8$, (ksi)	-0.3413×10^1	0.1728×10^0	-0.3429×10^{-3}
σ_{ult}, $[+30_2/-30_2]_s$ (MPa)	0.2320×10^3	0.5455×10^0	-0.1537×10^{-2}
σ_{ult}, $[+30_2/-30_2]_s$ (ksi)	0.3648×10^2	0.7912×10^{-1}	-0.2229×10^{-3}
σ_{ult}, $[+45_2/-45_2]_s$ (MPa)	0.7709×10^2	0.2747×10^0	-0.5211×10^{-3}
σ_{ult}, $[+45_2/-45_2]_s$ (ksi)	0.1118×10^2	0.3984×10^{-1}	-0.7558×10^{-4}
σ_{ult}, $[+60_2/-60_2]_s$ (MPa)	-0.1335×10^2	0.6392×10^0	-0.1156×10^{-2}
σ_{ult}, $[+60_2/-60_2]_s$ (ksi)	-0.1936×10^1	0.9270×10^{-1}	-0.1677×10^{-3}

4.0 SUMMARY

The results presented show that the elastic and strength properties of T300/5208 graphite-epoxy composite vary either linearly or quadratically with temperature. The important properties of longitudinal and transverse modulus (E_1 and E_2) show slight increases at both high and low temperatures. The remaining elastic properties exhibit a decrease with increasing temperature. Strength in the fiber-direction is linear with an increase in strength accompanied by an increase in temperature. All other strength measurements exhibit a second-order curve fit.

At elevated temperatures, reduced residual stresses result in lower matrix stresses and straighter fibers. Straighter fibers tend to improve the properties of the composite in the fiber direction, but have little effect in other directions. Therefore, the longitudinal modulus, E_1, and longitudinal strength, X_T, are increased while all other properties are affected very little.

At low temperatures, the epoxy matrix material becomes stiff and brittle. A stiffer matrix gives rise to increases in stiffness in all orientations of the composite. Strength is also increased in all cases except the 0°-material. A brittle and stiff matrix results in higher residual stresses and less efficient load transfer in regions of stress concentration, such as at fiber breaks, leading to decreased strength in the fiber direction.

Comparison between experimental and theoretical values for laminate modulus, for the 45°-laminate and the angle-ply laminates, indicates excellent agreement at room and elevated temperatures, but less than satisfactory agreement at the low temperature. This disagreement becomes worse with increasing fiber-angle. Possibly, the increase in

modulus and brittleness in the matrix material at lower temperatures has an affect on angle-ply laminates that is not taken into consideration with the classical lamination theory. More work will have to be done in this area to resolve this question.

ACKNOWLEDGEMENT

This work was supported by the NASA-Virginia Tech Composites Program under NASA grant CA-NCC1-15. The authors would also like to thank Peter Stein and Doug Wesley for their many hours spent assisting in the laboratory.

REFERENCES

1. Tenney, D. R., Sykes, G. F., and Bowles, D. E., "Space Environmental Effects on Materials," AGARD Conference Proceedings No. 327, Environmental Effects on Materials for Space Applications, papers presented at the 55th meeting of the AGARD Structures and Materials Panel in Toronto, Canada, on 19-24 September 1982.

2. Pindera, M. J. and Herakovich, C. T., "An Endochronic Theory for Transversely Isotropic Fiberous Composites," VPI-E-81-27, Virginia Polytechnic Institute and State University, October 1981.

3. Pindera, M. J. and Herakovich, C. T., "An Elastic Potential for the Nonlinear Response of Unidirectional Graphite Composites," Journal of Applied Mechanics, Vol. xx.

4. Hyer, M. W., Herakovich, C. T., Milkovich, S. M., and Short, J. S., "Temperature Dependence of Mechanical and Thermal Expansion Properties of T300/5208 Graphite-Epoxy," Composites, Volume 14, July 1983, pp. 276-280.

5. Curtis, G. J., Milne, J. M., and Reynolds. W. N., "Non-Hookean Behavior of Strong Carbon Fibers," Nature, Volume 220, December 1968, p. 1024.

6. Beetz, C. P., Jr., "Strain-Induced Stiffening of Carbon Fibres," Fibre Science and Technology, Volume 16, 1982.

7. Mansfield, E. H. and Purslow, D., "The Influence of Fiber Waviness on the Moduli of Unidirection Fiber Reinforced Composites," CP No. 1339, December 1974.

8. Bazant, Z. P., "Effect of Curvature of the Reinforcing Fibers on the Moduli of Elasticity and Strength of Composites," Polymer Mechanics, Volume 4, Number 2, 1968, pp. 251-258.

9. VanDreumel, W. H. M., and Kamp, J. L. M., "Non-Hookean Behavior in the Fibre Direction of Carbon-Fibre Composites and the Influence of Fibre Waviness on the Tensile Properties," J. Composite Materials, Volume 11, October 1977, p. 461.

10. Jones, R. M., Mechanics of Composite Materials, Scripta Book Company, Washington, DC, 1975, p. 66.

END

DATE

FILMED

AUG 10 1984